Surface acoustic wave investigations of the metal-to-insulator transition of V_2O_3 thin films on lithium niobate

C. Müller, A. A. Nateprov, G. Obermeier, et al.

View Online   Export Citation

ARTICLES YOU MAY BE INTERESTED IN

Surface acoustic wave investigations of the metal-to-insulator transition of V$_2$O$_3$ thin films on lithium niobate

C. Müller,[a] A. A. Nateprov, G. Obermeier, M. Klemm, R. Tidecks, A. Wixforth, and S. Horn
Institut für Physik, Universität Augsburg, Universitätsstrasse 1, D-86159 Augsburg, Germany

Thin V$_2$O$_3$ films were deposited on a piezoelectric substrate by electron-beam evaporation. Surface acoustic waves were generated by interdigital transducers. The attenuation and sound velocity were investigated from 260 to 10 K, providing an insight into the temperature-dependent electrical, dielectrical, and elastic properties of V$_2$O$_3$ at the metal-to-insulator transition. © *2005 American Institute of Physics*. [DOI: 10.1063/1.2103410]

I. INTRODUCTION

Vanadium oxide V$_2$O$_3$ shows a metal-to-insulator (MI) transition at $T_{MI} \approx 170$ K on cooling.[1–3] The electronic transition is accompanied by a structural change of the crystal lattice from trigonal to monocline. At the same time, a transition from a paramagnetic to an antiferromagnetic state is observed.[4]

Often V$_2$O$_3$ is regarded as a typical Mott-Hubbard system,[5–8] although the fact that the MI transition is accompanied by a structural transition complicates the situation.

Although the material has been studied extensively, the interplay of lattice as well as magnetic and electronic degrees of freedom has not yet been completely understood.[9–18] Probably due to the fact that the volume change at the transition easily destroys the crystals investigated, measurements of the elastic constants of V$_2$O$_3$ are scarce, but can be expected to contribute valuable information concerning the coupling of electronic and lattice degrees of freedom. For example, the compressible Hubbard model[19] predicts an anomaly of the sound velocity in V$_2$O$_3$ at the transition temperature.[20]

Thin films of V$_2$O$_3$ are not destroyed on passing the transition. The sound velocity of such a thin film can be measured using surface acoustic waves (SAW).[21] In this work we applied this technique to investigate the metal-to-insulator transition of V$_2$O$_3$ thin films on the piezoelectric substrate LiNbO$_3$ by measuring the attenuation and sound velocity as a function of temperature.

II. SAMPLE PREPARATION AND CHARACTERIZATION

Thin films of V$_2$O$_3$ of a thickness of $d = 370$ nm were produced in an ultrahigh-vacuum system by electron-beam evaporation from a V$_2$O$_3$ target onto a 128° rotated YX cut of a LiNbO$_3$ substrate. The target was prepared by sintering V$_2$O$_3$ powder (Chempur) under pressure in a reducing atmosphere.

The film thickness was determined *ex situ* by a Dektak profilometer. The films show a typical grain size of about 15–25 nm, as inferred from atomic force microscopy (AFM). An image is shown in Fig. 1.

X-ray-diffraction (XRD) measurements carried out in the $\Theta/2\Theta$ mode with Θ ranging from 35° to 65° (Fig. 2) show the (110), (113), (116) Bragg peaks of V$_2$O$_3$.[22,23] The fact that no other V$_2$O$_3$ peaks are observed indicates a partially textured structure of the film. The other Bragg peaks seen in Fig. 2 originate from the LiNbO$_3$ substrate, the metallic IDTs, and the aluminum sample holder. From the peak positions, a reduction of the c parameter by $\sim 0.5\%$ compared to bulk V$_2$O$_3$[22,18] is estimated. Within the margins of error, the a parameter is that of bulk material. For this analysis, the shift ($\sim 0.2°$) of the peaks due to the thickness of the sample is taken into account.

III. MEASURING TECHNIQUES

Interdigital transducers (IDTs), which are microstructured finger electrodes made of aluminum, were used to measure the sound velocity and the attenuation of surface acoustic waves.[21]

The IDTs were placed on a LiNbO$_3$ piezoelectric substrate (Fig. 3). The 128° rotated YX cut (i.e., propagation of the SAW in the X direction) used has a high electromechanical coupling constant, $K^2 = 0.056$,[24] which relates the electrical to the total wave energy density, and is a measure for the
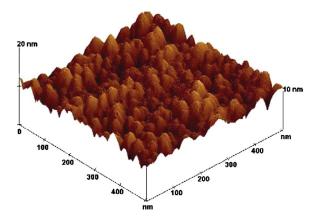

FIG. 1. AFM image of a V$_2$O$_3$ thin film deposited on LiNbO$_3$.

[a]Author to whom correspondence should be addressed; electronic mail: claus.mueller@physik.uni-augsburg.de
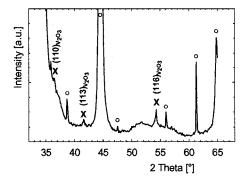
FIG. 2. XRD measurements of a V_2O_3 thin film ($d=370$ nm) deposited on $LiNbO_3$. X: V_2O_3 peaks; o: Substrate and sample holder peaks.

electrical interaction strength of the SAW with the film on top, as is obvious from Eqs. (2) and (4) below.

The length of the V_2O_3 film was $L_F=4.18$ mm, its width $w=(2.7\pm0.1)$mm. The bond contacts for the dc measurements (Al wires, diameter 50 μm, resulting in a bond contact area of typically $\sim$90 μm) were arranged near to the lower border of the film. The current leads were placed at $\sim$0.85 mm and $\sim$0.25 mm from the left and right corner, respectively. The voltage probes (distance $L=200$ μm, midpoint to midpoint) were situated approximately in the middle between the current leads.

The IDTs are centered at $\sim w/2$ of the V_2O_3 film, extending over about 25% of the width. The distance between the IDTs and the film is$\sim$0.35 and 0.47 mm at the left and right side, respectively.

The transducer emitted a SAW of a certain wavelength λ defined by the spacing of the finger electrodes. As we used split-4 finger electrodes (i.e., every finger sketched in Fig. 3 consists of four separated metallic lines of distances 4.33 μm midpoint), $\lambda=8\times4.33$ μm$=34.64$ μm, which is equal to the quantity b in Fig. 3. The best emitted frequency, the so called fundamental frequency f_0, is then given by

$$\lambda f_0 = v_0 \tag{1}$$

Here, $v_0=3978.2$ m/s is the sound velocity of 128° rot. YX $LiNbO_3$ at room temperature.[25]

To excite the SAW electrically, a radiofrequency voltage with the fundamental frequency of the IDT (typically 112 MHz) was supplied to one of the IDTs.

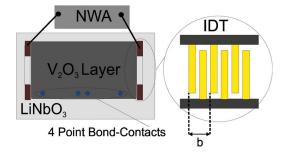The SAW propagating along the substrate from the sending IDT to the identical receiving IDT (i.e., along the "sound

FIG. 3. Schematic view of a surface acoustic transmission line: A V_2O_3 film on top of $LiNbO_3$ together with an enlarged view of the IDT structure. Bond contacts serve for dc resistivity measurements.

path" or "delay line"), where it is detected electrically, has an electrical and a mechanical part due to the piezoelectricity of $LiNbO_3$. The overall attenuation of the applied and detected electrical radiofrequency signal was determined by a vector network analyzer (NWA) (ZVC Rohde und Schwarz). The sound path $\Delta_{IDT,EFF}$ is about 5.5 mm, considering the length of the IDTs in addition to their distance, as concluded from the sound velocity v_0 and the propagation time of the SAW from IDT to IDT for $LiNbO_3$.

As the IDT structure behaves like a bandpass filter, it is essential to measure the attenuation at the frequency f_0, which is transmitted best. Otherwise, one gets an apparent attenuation contribution coming from the filter characteristics. To avoid this contribution, the frequency with the lowest attenuation was tracked during the whole measurement (tracking range $\sim$109 -117 MHz) and taken as the fundamental frequency.

We defined a certain frequency range which contained the fundamental frequency f_0. Now the attenuation at 501 equidistant frequency points was measured by the network analyzer. However, the attenuation at these frequencies contains not only the signal of the SAW but also a contribution from a direct electromagnetic coupling of the two IDTs. By Fourier transformation of the measured frequency spectrum, one can get the information in the time domain. Here it is possible to distinguish between the direct electrical crosstalk received by the second IDT in between nanoseconds and the SAW signal arriving after around 1 μs. By setting a time gate, it is possible to suppress the signal not arising from the SAW. Transforming back the gated data into the frequency domain yields the attenuation containing information of the SAW signal only. Then the attenuation at the fundamental frequency was read out from the NWA.

With a second independent channel of the NWA, the group velocity [which is equal to the phase velocity as long as Eq. (1) holds] was measured by taking the propagation time of the SAW at the minimal transmitted attenuation in the time domain. Then the velocity can be calculated, as the distance $\Delta_{IDT,EFF}$ between the IDTs is known.

Measurements between 260 and 10 K were performed in a cryostat (American Magnetics) with a variable temperature insert (VTI). Because the temperature is lowered, the spacing b (see Fig. 3) between the finger electrodes of the IDTs and, therefore, the wavelength λ of the emitted SAW also decreases. Additionally, the sound velocity v_0 of the $LiNbO_3$ in principle may vary with temperature. Equation (1) shows that then the fundamental frequency f_0 changes. Thus, the attenuation minimum had to be tracked during the whole measurement.

In parallel to the SAW studies, resistivity measurements of the film were carried out. A four-point method with a constant current source (Keithley 2400) and a multimeter (Keithley 2000) measuring the voltage was used. The resistance of the film (Fig. 4) was calculated from the measured voltage and the actual value of the current (10 μA as long as the current source could impress a constant current). For a resistance higher than $\sim$3 MΩ the data became noisy, i.e., they are no longer reliable and are, therefore, omitted.

Measurements of an empty $LiNbO_3$ substrate not cov-

FIG. 4. Temperature dependence of the resistance and sheet conductance $\sigma_\square$, respectively, of a V_2O_3 film on $LiNbO_3$ substrate.

ered with a V_2O_3 film yield an attenuation of $\sim$18 dB over the whole temperature range investigated. Moreover, there is almost no (for a detailed discussion see below) change in the sound velocity.[26]

IV. RESULTS AND DISCUSSION

The measured dc resistance and the sheet conductance, respectively, are displayed in Fig. 4. The jump in the resistivity at the metal-to-insulator transition amounts to at least six orders of magnitude. A lower transition temperature as observed for the MI transition of the films compared to stoichiometric bulk material [T_{MI}=170 K (Ref. 18)] is expected for a reduced c parameter of the film, as inferred from XRD. The hysteresis observed between cooling and warming is slightly wider than that for a single crystal of similar transition temperature.[27]

The temperature-dependent attenuation signal of the SAW measurement (Fig. 5) also shows a hysteretic behavior. On cooling, the maximum of the SAW attenuation (75 dB) appears at 98 K, while increasing the temperature leads to a maximum ($\sim$95 dB) at 115 K. The noise at around 10 K may be due to adsorption of helium on the V_2O_3 film, resulting in an additional damping of the SAW. At higher temperatures there is a continuous decrease of the baseline.

To describe the interaction of the SAW with the V_2O_3 layer, the theory of Ingebrigtsen[28] was applied, originally
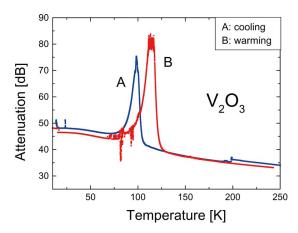

FIG. 5. SAW attenuation as a function of temperature.

developed to describe a piezoelectric material coated with a semiconducting film. Starting from Eq. (2.16) of Ref. 28 (valid if the film thickness d is small compared to the acoustic wavelength, i.e., $kd \ll 1$, with $k=2\pi/\lambda$ the wave number of the SAW) a straightforward calculation yields the absorption coefficient,

$$\Gamma = K^2 \frac{\pi}{\lambda} \frac{\eta \gamma \sigma_\square / \sigma_m}{\eta^2 + (\sigma_\square / \sigma_m)^2}. \quad (2)$$

Here, K^2 is the electromechanical coupling constant, $\eta = 1 - (v_D/v_0)$, with v_D the carrier drift velocity, v_0 the phase velocity of the SAW, and $\gamma = \varepsilon_p/(\varepsilon_p + \varepsilon_0)$, with ε_p the effective dielectric constant for the piezoelectric, ε_0 the permittivity, and λ the wavelength of the SAW. Moreover, $\sigma_\square$ is the sheet conductance of the film and $\sigma_m = v_0(\varepsilon_p + \varepsilon_0) = v_0 \varepsilon_0 (\varepsilon_p/\varepsilon_0 + 1)$.

For $v_D \ll v_0$ and $\varepsilon_p \gg \varepsilon_0$ so that $\eta \sim 1$ and $\gamma \sim 1$, one gets

$$\Gamma = K^2 \frac{\pi}{\lambda} \frac{\sigma_\square / \sigma_m}{1 + (\sigma_\square / \sigma_m)^2}. \quad (3)$$

According to Refs. 25 and 29, Eq. (3.8), it is $\varepsilon_p = \varepsilon_0(\varepsilon_{11}\varepsilon_{33} - \varepsilon_{13}^2)^{1/2}$, with $\varepsilon_{11}, \varepsilon_{33}$, and ε_{13} the direction-dependent dielectric constants of $LiNbO_3$ (tensor elements) at constant stress conditions.[30]

Following Ref. 24, we have $\varepsilon_p + \varepsilon_0 = C_s$, with C_s = 5 pF/cm for the 128° rotated YX cut of $LiNbO_3$, yielding $\sigma_m = 2 \times 10^{-6} \Omega^{-1}$.

The sheet conductance is obtained from the measured dc resistance R of the V_2O_3 film by $\sigma_\square = R_\square^{-1} = d/\rho$, where the resistivity of the film is $\rho = Rwd/L$, with w the width of the film and L the distance of the voltage probes, yielding $\sigma_\square = (L/w)R^{-1}$.

The absorption coefficient Γ becomes maximal for $\sigma_\square = \sigma_m$ resulting in $\Gamma(\sigma_m) = K^2 \pi/2\lambda$.

A change of the sheet conductance of the coating film results in a change of the sound velocity v. With $\Delta v = v - v_0$, the normalized sound velocity shift is given by

$$\frac{\Delta v}{v_0} = \frac{K^2}{2} \frac{1}{1 + (\sigma_\square / \sigma_m)^2}. \quad (4)$$

To obtain this equation, we consider the results of Hutson and White[31] for the absorption coefficient and the change of the sound velocity of an elastic wave in a homogeneous piezoelectric semiconductor. In the case in which the diffusion terms of the charge carriers are neglected, the expression for Γ is in formal analogy to Eq. (3) of the present work, derived from the paper of Ingebrigtsen.[28] However, in the results of Ref. 31, the ratio ω_c/ω appears instead of $\sigma_\square/\sigma_m$, with ω_c the angular frequency of the relaxation of a perturbation of the electron density.[32] Thus, Γ as given by Hutson and White transforms to an absorption coefficient for a SAW in a piezoelectric material coated with a conducting film [Eq. (3)], when ω_c/ω is replaced by $\sigma_\square/\sigma_m$. If we carry out the same substitution in the expression for the change of the sound velocity of Ref. 31, we obtain Eq. (4) of the present work, in agreement with Ref. 33, in which the same result is obtained from Hutson and White by a different transformation procedure.
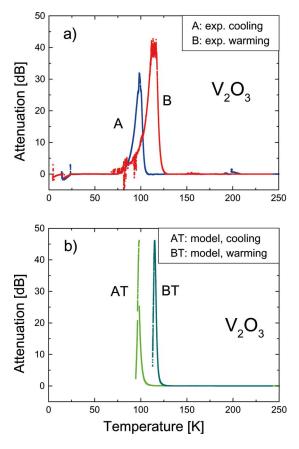
FIG. 6. Comparison of experimental (a) and calculated values (b) for the attenuation of the SAW.

If the surface of the SAW device is covered with a thin metal film, the electric field of the SAW is short-circuited and the piezoelectric material becomes softer due to the missing electrical restoring forces.

The relation between the short-circuited sound velocity, v_{sc}, and open sound velocity v_0, and the electromechanical coupling constant K^2 is given by[34]
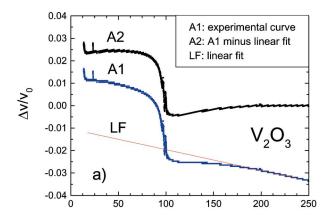
$$v_{sc} = v_0(1 - K^2/2). \tag{5}$$
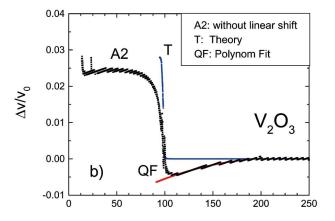
Thus, the normalized sound velocity shift is

$$(v_{sc} - v_0)/v_0 = K^2/2 = 0.028. \tag{6}$$

For a quantitative comparison of the measured attenuation with the theory, one has to consider that the electrical signal associated with the SAW in LiNbO$_3$ between the sending IDT and the receiving IDT decreases by a factor $F = \exp(-\Gamma L_F)$. The attenuation in dB units is, thus, given by $10 \log F^2 = 20 \log F$. The absorption coefficient Γ in the expression for F can be calculated according to Eq. (3), using the measured dc sheet conductance of Fig. 4. This theoretical prediction for the attenuation is displayed in Fig. 6(b).

In Fig. 6(a), the attenuation data of Fig. 5 are plotted after a removal of the baseline, which decreases with increasing temperature. In this representation, the shape of the measured attenuation is similar to the calculated one.

The maxima of the attenuation in Figs. 6(a) and 6(b) appear at the same positions. To achieve this, we took the values $\sigma_m = 2.5 \times 10^{-6}\ \Omega^{-1}$ (cooling) and $\sigma_m = 0.5 \times 10^{-6}\ \Omega^{-1}$ (warming), respectively, as observed for the dc
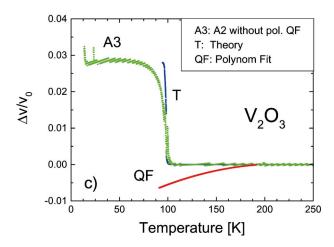

FIG. 7. Velocity shift vs temperature for cooling down.

sheet conductance (Fig. 4) at the temperature of the respective maxima of the attenuation. The difference in σ_m may be due to a change of the relative permittivity of the V$_2$O$_3$ film or a percolation of the current in the dc conductivity measurement with different paths for increasing and decreasing temperature. However, the values for σ_m are both in the order of magnitude expected for LiNbO$_3$ given above.

As the temperature range of the dc resistance measurement (Fig. 4) does not extend over the whole temperature range of the attenuation measurement, the temperature range covered by the calculation, which uses as an input the resulting sheet conductance, is also limited.

The sound velocity shift $\Delta v = v - v_0$ due to the V_2O_3 film normalized to v_0 is plotted in Fig. 7. Curve A1 shows the normalized measured sound velocity shift on cooling. In the temperature regions around 240 and 30 K, respectively, an increase of the velocity shift with decreasing temperature, which can be approximated by a linear fit (LF) with the slope 9.23×10^{-5} K^{-1}, is observed. It is of the same order of magnitude as the sound velocity shift of $LiNbO_3$ without film of about 6×10^{-5} K^{-1}. Subtracting this linear contribution from curve A1 yields curve A2.

Next, we plotted the sound velocity as calculated by Eq. (4) (curve T, input σ_m and $\sigma_\square$ as determined from the dc resistance). At around 200 K, the data of curve A2 start to deviate from curve T. The deviation can be fitted by a polynomial of second order (QF). This polynomial was then subtracted from curve A2 only in the temperature range (200–115 K), where the curve bends down contrary to the prediction of the model, yielding curve A3. QF represents an additional contribution not taken into account in Eq. (4).

It is remarkable that the step height of curve A3 is equal to the expected height (curve T), which is the difference of the velocities of $LiNbO_3$ covered with insulating and highly conducting thin layers, respectively, expressed by Eq. (6).

It also should be noted that for lower temperatures the measured increase of the sound velocity is smoother than the theoretically predicted jump. This has its equivalence in the broad shoulder of the measured attenuation data of Fig. 6.

In the dc resistance (and consequently also in the calculated attenuation and the velocity shift), there are jumplike changes close to the maxima of the attenuation. This phenomenon is an intrinsic property of the sample, occurring at decreasing temperature. In a larger magnification, not only a steplike change of the dc resistance is observed, but also a change of the slope of the curve. The reason for this behavior is not clear. A possible explanation could be cracks in the V_2O_3 film due to stress, induced by the structural change connected with the metal-to-insulator transition.

V. CONCLUSIONS

Thin films of V_2O_3 showing a metal-to-insulator transition were deposited on a piezoelectric substrate ($LiNbO_3$). The attenuation and the sound velocity shift of a surface acoustic wave interacting with the V_2O_3 film were measured in a temperature range between 260 and $\sim$10 K.

Using independently measured values for the dc sheet conductance at the maxima of the attenuation, agreement between the measured and calculated temperature of the maxima could be obtained. The shape of the calculated attenuation is only in qualitative agreement with the measurement. Quantitatively, the height of the maxima and especially the width differ. This suggests that a model based exclusively on the conductance of the V_2O_3 film is not sufficient to explain the behavior close to the metal-to-insulator transition.

In the sound velocity shift, a softening seems to occur already 60 K above the resistance jump. This cannot be explained by the simple model of a piezoelectric material coated with a thin film, on which Eq. (4) is based. This softening could possibly be due to an interplay between or-bital and lattice degrees of freedom. This behavior may be regarded as a precursor of the metal-to-insulator phase transition, as recently proposed to interpret extended x-ray absorption fine structure (EXAFS) measurements on V_2O_3.[35]

To our knowledge, the only experimental investigation of the metal-to-insulator transition of V_2O_3, which applied SAW before, has been performed on thin films deposited on Al_2O_3 and single crystals by Boborykina *et al.*[36] However, the V_2O_3 films were not directly deposited onto the piezoelectric substrate on which the SAW was excited but clamped to its surface. This is the main difference compared to the experiments in the present paper. Moreover, a different measuring technique was used. The attenuation as well as the normalized velocity shift are two orders of magnitude smaller and show a much less pronounced shape compared to the measurements of the present work. The normalized sound velocity in that paper in contrast to the present work decreases for temperatures below the metal-to-insulator transition. To get agreement between theory and experiment of the maximal attenuation, a higher sheet conductance σ_m has to be assumed compared to the known value of $LiNbO_3$.

Finally, it should be noted that only a direct deposition of V_2O_3 on the piezoelectric substrate as performed in the present work opens the possibility of device applications.

[1]M. Foëx, C. R. Hebd. Seances Acad. Sci. **223**, 1126 (1946).
[2]J. F. Morin, Phys. Rev. Lett. **3**, 34 (1959).
[3]W. Brückner, H. Oppermann, W. Reichelt, J. I. Terukow, F. A. Tschud-nowski, and E. Wolf, *Vanadiumoxide* (Akademie, Berlin, 1983).
[4]D. B.McWhan, A. Menth, J. P. Remeika, W. F. Brinkmann, and T. M. Rice, Phys. Rev. B **7**, 1920 (1973).
[5]N. F. Mott, Rev. Mod. Phys. **40**, 677 (1968).
[6]D. B. McWhan, T. M. Rice, and J. P. Remeika, Phys. Rev. Lett. **23**, 1384 (1969).
[7]M. Imada, A. Fujimori, and Y. Tokura, Rev. Mod. Phys. **70**, 1039 (2003).
[8]K. Held, G. Keller, V. Eyert, D. Vollhardt, and V. I. Anisimov, Phys. Rev. Lett. **86**, 5345 (2001).
[9]J. B. Goodenough, *Proceedings of the Tenth International Conference on the Physics of Semiconductors* (Atomic Energy Commission, Oak Ridge, 1970), p. 304.
[10]O. Müller, J. P. Urbach, E. Goering, T. Weber, R. Barth, H. Schuler, M. Klemm, S. Horn, and M. L. denBoer, Phys. Rev. B **56**, 15056 (1997).
[11]J.-H. Park, L. H. Tjeng, A. Tanaka, J. W. Allen, C. T. Chen, P. Metcalf, J. M. Honig, F. M. F. de Groot, and G. A. Sawatzky, Phys. Rev. B **61**, 11506 (2000).
[12]F. Mila, R. Shiina, F.-C. Zhang, A. Joshi, M. Ma, V. Anisimov, and T. M. Rice, Phys. Rev. Lett. **85**, 1714 (2000).
[13]R. J. Radwanski and Z. Ropka, cond-mat/0012257.
[14]R. Shiina, F. Mila, F.-C Zhang, and T. M. Rice, Phys. Rev. B **63**, 144422 (2001).
[15]E. Goering, M. Schramme, O. Müller, R. Barth, H. Paulin, M. Klemm, M. L. den Boer, and S. Horn, Phys. Rev. B **55**, 4225 (1997).
[16]A. Tanaka, J. Phys. Soc. Jpn. **71**, 1091 (2002).
[17]A. Tanaka, Physica B **329-333**, 753 (2003).
[18]S. Klimm, M. Herz, R. Horny, G. Obermeier, M. Klemm, and S. Horn, Phys. Rev. B **64**, 184435 (2001).
[19]P. Majumdar and H. R. Krishnamurthy, Phys. Rev. Lett. **73**, 1525 (1994).

[20]S. R. Hassan, A. Georges, and H. R. Krishnamurthy, Phys. Rev. Lett. **94**, 036402 (2005).

[21]R. M. White and F. W. Voltmer, Appl. Phys. Lett. **7**, 314 (1965).

[22]Landolt-Börnstein Neue Serie III/17g, *Semiconductors: Physics of Non-Tetrahedrally Bonded Binary Compounds III* (Springer, Berlin, 1984).

[23]Calculation of the peak position via the Powder Cell 2.01 program.

[24]S. Datta, *Surface Acoustic Wave Devices* (Prentice-Hall, Englewood Cliffs, NJ, 1986), Table 3.2.

[25]G. Kovacs, M. Anhorn, H. E. Engan, G. Visintini, and C. C. W. Ruppel, Proc.-IEEE Ultrason. Symp. 435-438 (1990).

[26]A. Hörner (private communication).

[27]S. Klimm, Magnetotransportmessungen zur Untersuchung der elektronischen Struktur von V_2O_3 und MoO_2, Dissertation, Universität Augsburg (Shaker Verlag, Aachen, 1997).

[28]K. A. Ingebrigtsen, J. Appl. Phys. **41**, 454 (1970).

[29]K. A. Ingebrigtsen, J. Appl. Phys. **40**, 2681 (1969).

[30]*Landolt-Börnstein: Ferroelektrika und verwandte Substanzen* (Springer, Berlin, 1981), Vol. 16.

[31]A. R. Hutson and D. L. White, J. Appl. Phys. **33**, 40 (1962).

[32]S. V. Biryukov, Yu. V. Gulyaev, V. V. Krylov, and V. P. Plessky, *Surface Acoustic Waves in Inhomogeneous Media, Wave Phenomena* (Springer, Berlin, 1995), Vol. 20.

[33]A. Wixforth, J. Scriba, M. Wassermeier, J. P. Kotthaus, G. Weimann, and W. Schlapp, Phys. Rev. B **40**, 7874 (1989).

[34]H. Matthews, *Surface Wave Filters* (Wiley, New York, 1977).

[35]P. Pfalzer, Lokale strukturelle und elektronische Eigenschaften von V_2O_3 und ZnV_2O_4, Dissertation, Universität Augsburg (2004), Chaps. 5.2.4 and 8.1.

[36]E. N. Boborykina, S. E. Nikitin, and F. A. Chudnovskii, Rus. Ultas. **25**, 275 (1995).